INTERNATIONAL JOURNAL OF CLIMATOLOGY
Int. J. Climatol. (2013)
Published online in Wiley Online Library
(wileyonlinelibrary.com) DOI: 10.1002/joc.3839

RMetS
Royal Meteorological Society

The change of cherry first-flowering date over South Korea projected from downscaled IPCC AR5 simulation

Jina Hur,[a] Joong-Bae Ahn[a]* and Kyo-Moon Shim[b]

[a] *Division of Earth Environmental System, Pusan National University, Busan, Republic of Korea*
[b] *National Academy of Agricultural Science, RDA, Suwon, Republic of Korea*

ABSTRACT: Simulations from six global climate models participating in Coupled Model Intercomparison Project 5 are used to project future changes in regional early spring (February–April) temperature and in cherry (*Prunus yedoensis*) first-flowering date (FFD) over South Korea in order to investigate a potential plant growth response to local climate change. For the study, we statistically downscale daily Historical (1986–2005), RCP4.5 (2071–2090), and RCP8.5 (2071–2090) gridded model data to 59 cherry FFD observation sites over South Korea. In order to reduce the uncertainties in the model simulation produced by a single model, multi-model ensemble (MME) is performed after eliminating the mean systematic bias of each model. A shift of cherry FFD under global warming is estimated and compared with the observation and Historical simulation by applying the downscaled data to a DTS phenological model. The analysis reveals a projected advance in cherry FFD over South Korea by 2090 of 6.3 and 11.2 days compared to the current dates due to a rising mean temperature of about 2.0 and 3.5 K under the RCP4.5 and RCP8.5 scenarios, which approximately correspond to moving north at a speed of 0.01 and 0.03°N year^{-1}, respectively. These average yearly advances (0.07 and 0.13 days year^{-1}) of cherry FFD in the RCP4.5 and RCP8.5 simulations are 0.22 and 0.16 days year^{-1} lower, respectively, than the value of 0.29 days year^{-1} derived in previous studies with the SRES A2 scenario. Regardless of the difference between the SRES A2 and RCP8.5 scenarios, the discrepancy in the advancement tendency was primarily attributed to the inability of the previous studies to eliminate the systematic model biases, which led to overestimation of both the temperature and the FFD changes.

KEY WORDS AR5 simulations; RCP scenarios; cherry first-flowering date; temperature projection; statistical downscaling

Received 13 March 2013; Revised 19 July 2013; Accepted 10 September 2013

1. Introduction

The concentrations of greenhouse gases such as CO_2, CH_4, and N_2O have been rapidly increasing since the 1750s because of anthropogenic activities. This increase has strengthened the greenhouse warming effect and consequently increased the global surface air temperature by $0.6 \pm 0.2\,^{\circ}C$ in the last century (Intergovernmental Panel on Climate Change, IPCC, 2007a).

Global warming induces climate changes in a wide range of spatial and temporal spectra in the climate system through the complex physical and dynamical interactions and feedbacks within the system. Recently, biospheric responses to climate change, such as changes in ecosystem and agriculture, have attracted the interest of many scientists (e.g. Ho *et al.*, 2006; IPCC, 2007a). In particular, plant and crop phenologies such as time of leafing, flowering, and fruiting, which respond sensitively to climatic conditions, have been regarded as integral biological indicators, along with air temperature and CO_2 concentration. They have been studied in order to estimate the effect of climate change on the growth and development of plants and crops (Ho *et al.*, 2006; Yun, 2006; Aono and Kazui, 2008; Chung *et al.*, 2009; Ohashi *et al.*, 2012).

Rapid warming has been observed over South Korea for the last several decades, as in other mid- and high-latitudinal areas, particularly during winter and spring (Jung *et al.*, 2002; Oh *et al.*, 2004; Kwon, 2005). The flowering date for deciduous trees in mid- and high-latitude, in particular, depends strongly on the temperature of winter and early spring among several climate factors (Menzel and Fabian, 1999; Wielgolaski, 2003). For example, the flowering date of cherry trees over South Korea is strongly influenced by the temperature for 3 months from February to April (Jeong *et al.*, 2011). Accordingly, many studies (e.g. Yun, 2006; Chung *et al.*, 2009; Jeong *et al.*, 2011) have been performed to project the changes of spatial distribution of the flowering time for certain fruit trees in association with regional climate change. Among deciduous trees, the cherry tree (*Prunus yedoensis*), which flowers in early spring, is widely distributed throughout the Korean Peninsula. The flowering time of the cherry blossom has been observed by Korean meteorological observation sites since 1922 and these flowering data have, therefore, been usefully applied by

* Correspondence to: J.-B. Ahn, Division of Earth Environmental System, Pusan National University, Pusan 609735, Republic of Korea.
E-mail: jbahn@pusan.ac.kr

many phenological studies (Jung *et al.*, 2005; Ho *et al.*, 2006; Yun 2006; Chung *et al.*, 2009; Jeong *et al.*, 2011). Among these studies, Chung *et al.* (2009) and Yun (2006) estimated the flowering time of the cherry blossom using high-resolution regional surface air temperature obtained from monthly mean projection data based on AR4 climate scenario. Their studies, however, did not consider the daily temperature variation in the estimation. Instead, the daily temperatures were statistically obtained from the monthly mean data of a climate prediction model. In addition, these estimations are believed to contain some uncertainties because the authors used only a single climate prediction model result and, further, did not correct its mean bias in their studies. Their studies compared SRES A2 simulations (2011–2100) directly with observation (1971–2000), without applying any bias corrections. The resulting bias of the model may have induced incorrect climate change signal. Therefore, the elimination of the systematic bias is important in understanding and estimating the cherry first-flowering date (FFD).

In this study, based on the AR5 climate scenarios of Historical (1986–2005), RCP4.5 (2071–2090), and RCP8.5 (2071–2090) simulations, the FFD of the cherry blossom in South Korea is newly estimated using daily temperature data obtained from six different climate models. In order to reduce uncertainties (Krishnamurti *et al.*, 1999; Yun *et al.*, 2003; Ahn *et al.*, 2012), multi-model ensemble (MME) results are used after removing the mean bias of individual models.

2. Data and method

2.1. Climate change data

In order to examine temperature changes resulting from a variety of radiative forcing, we use the RCP4.5 and RCP8.5 climate scenarios with radiative forcing of 4.5 and 8.5 W/m^2, which are similar to SRES B1 and SRES A2 or A1F1 of AR4, respectively (IPCC, 2007a, 2007b; Lamarque *et al.*, 2011; van Vuuren *et al.*, 2011). The data used are daily Historical (1986–2005), RCP4.5 (2071–2090), and RCP8.5 (2071–2090) gridded temperature for early spring (February–April, FMA) from six models participating in the Coupled Model Intercomparison Project 5 (CMIP5). This 'early spring' is selected and defined by considering the positive relationship between temperature and cherry FFD, based on the results of Jeong *et al.* (2011). The 6-Coupled General Circulation Models (6-CGCMs), the details of which are presented in Table 1, are chosen because their horizontal resolutions are less than 200 km.

The gridded data having relatively coarse resolution simulated by the global climate models are statistically downscaled to *in-situ* meteorological observation sites in South Korea. For the statistical downscaling, we use a hypsometric method that considers both inverse distance weighting and the lapse rate correction factor based on elevation difference (Dodson and Marks, 1997; Daly *et al.*, 2003). The topographic effect is reflected in the downscaled data as follows:

$$\mathrm{Ts} = \frac{\sum_{i=1}^{n} \frac{\mathrm{Tm}_i}{d_i^2}}{\sum_{i=1}^{n} \frac{1}{d_i^2}} + \left[\mathrm{Zs} - \frac{\sum_{i=1}^{n} \frac{\mathrm{Zm}_i}{d_i^2}}{\sum_{i=1}^{n} \frac{1}{d_i^2}} \right] \Gamma \qquad (1)$$

$$\Gamma = -1 \times |0.00688 + 0.0015 \times \cos\left(0.0172\,(\text{Julian day} - 60)\right)| \qquad (2)$$

Here, Ts and Zs indicate the temperatures and altitudes at 59 observation sites over South Korea (Figure 1), respectively, and Γ is the empirical lapse rate with altitude (Yun *et al.*, 2000). Tm_i and Zm_i are defined as the temperature and altitude at the ith grid point among n grid points within the influence radius from the *in-situ* observation site. The radiuses of influence for BCC-CSM1-1M, CCSM4, CMCC-CM, EC-EARTH, MIROC5, and MRI-CGCM3 are set as 79, 75, 53, 79, 99, and 79 km, respectively, which are half of the average distance of each model's resolution.

The simulated temperatures over the Northern Hemisphere and Northeast Asia are compared with the National Centers for Environmental Prediction/National Center for Atmospheric Research (NCEP/NCAR) reanalysis 2 (hereafter NCEP2) (Kanamitsu *et al.*, 2002) data. The mean bias of each model downscaled to the observation sites is estimated and eliminated using daily temperature during the 20-year period from 1986 to 2005 obtained from the 59 *in-situ* observations over South Korea. In addition, MME is performed using the Simple Composite Method in order to produce a representative value for each scenario and to reduce uncertainties contained in individual models (Krishnamurti *et al.*, 1999; Yun *et al.*, 2003).

2.2. Cherry flowering data

The cherry FFD data observed by the Korean Meteorological Administration are used to analyse the current characteristics of cherry FFD and to verify the capability of FFD simulation. Figure 1 shows the distribution of the 59 observation sites for temperature and cherry FFD over South Korea.

Several phenological models such as a temperature accumulation model using the number of days transformed to standard temperature (DTS) model (Ono and Konno, 1999), two-step model based on growing degree days (Yun, 2006; Chung *et al.*, 2009), and statistical model (Menzel and Dose, 2005) have been developed and adopted for cherry FFD estimation. Aono and Kazui (2008) claimed that the accuracy given by the DTS model is generally higher than that given by some other common approaches. Therefore, DTS is applied to the downscaled

Table 1. Description of six CGCMs participating in CMIP5 is used in this study.

Model acronym	Institution	Resolution (lon × lat)	Reference
BCC-CSM1-1M	Beijing Climate Center, China Meteorological Administration	320 × 160	Wu *et al.* (2010)
CCSM4	National Center for Atmospheric Research	288 × 192	Gent *et al.* (2011)
CMCC-CM	Centro Euro-Mediterraneo per I Cambiamenti Climatici	480 × 240	Scoccimarro *et al.* (2011)
EC-EARTH	EC-EARTH consortium	320 × 160	Hazeleger *et al.* (2010)
MIROC5	Atmosphere and Ocean Research Institute (The University of Tokyo), National Institute for Environmental Studies, and Japan Agency for Marine-Earth Science and Technology	156 × 128	Watanabe *et al.* (2010)
MRI-CGCM3	Meteorological Research Institute	320 × 160	Mizuta *et al.* (2012) and Yukimoto *et al.* (2011)

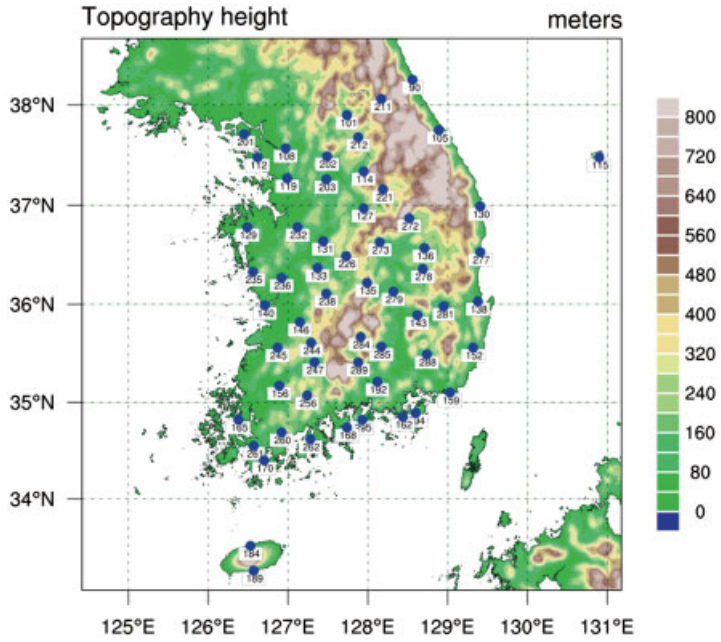

Figure 1. Locations of 59 weather stations (blue dots) used to observe temperature and cherry flowering date and topography (shaded, m) of South Korea.

climate model output for the study as follows:

$$\sum_{i=1}^{n\text{day}} (\text{dailyDTS})_i = \sum_{i=1}^{n\text{day}} \left(\exp \left\{ \frac{E_a (T_i - T_s)}{R \bullet T_i \bullet T_s} \right\} \right) \quad (3)$$

where T_i is the mean temperature at the ith day from the starting day of daily DTS accumulation, T_s the standard temperature (288.2 K), R the ideal gas constant (8.314 J K^{-1} mol^{-1}), and E_a the sensitivity of plant to temperature. In order to use the DTS method, three constants for the cherry blossom over South Korea are selected (Ono and Konno, 1999): (1) Ds: starting day of calculation (Julian day; JD), (2) E_a: temperature sensitivity (kJ mol^{-1}), and (3) DTS: accumulated daily DTS from Ds day to cherry FFD. By applying a combination of the three constants to the observed temperature, we select the fittest combination of constants representing the observed cherry FFD.

3. Results and discussions

3.1. Change of temperature over Northeast Asia

First, the temperature over Northeast Asia derived from the six climate models and the reanalysis data are investigated and compared (Figure 2). According to the NCEP2 reanalysis, the temperatures around the Korean peninsula are relatively lower than those of the surrounding area, and show a decreasing trend with increasing latitude. The general patterns of the historical simulations are similar to the NCEP2 reanalysis, although they differ from the analysis by between −0.5 and 1.6 K, which are attributed to systematic bias (Ahn *et al.*, 2012) caused by incompleteness in the model's boundary and initial conditions, physical and subgrid-scale parameterizations, etc. Hence, such systematic bias should be eliminated before using the value for analysis and application (Ahn *et al.*, 2010).

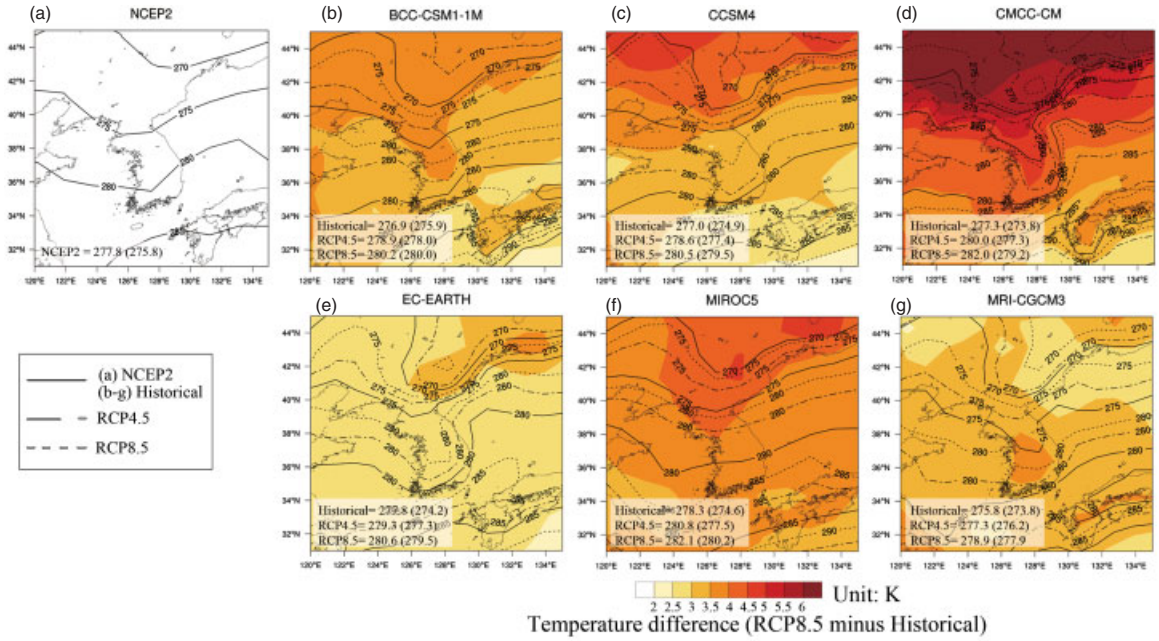

Figure 2. Average temperature (K) derived from NCEP reanalysis 2 data (for 1986–2005, a), Historical (for 1986–2005, solid line), RCP4.5 (for 2071–2090, dash-dotted line), and RCP8.5 (for 2071–2090, dotted line) simulations (b–g) for the flowering period (February–April). The left and right values in the bottom-left are the mean temperatures over Northeast Asia and the Northern Hemisphere, respectively. Here shading indicates the temperature difference between the Historical and RCP8.5 simulations.

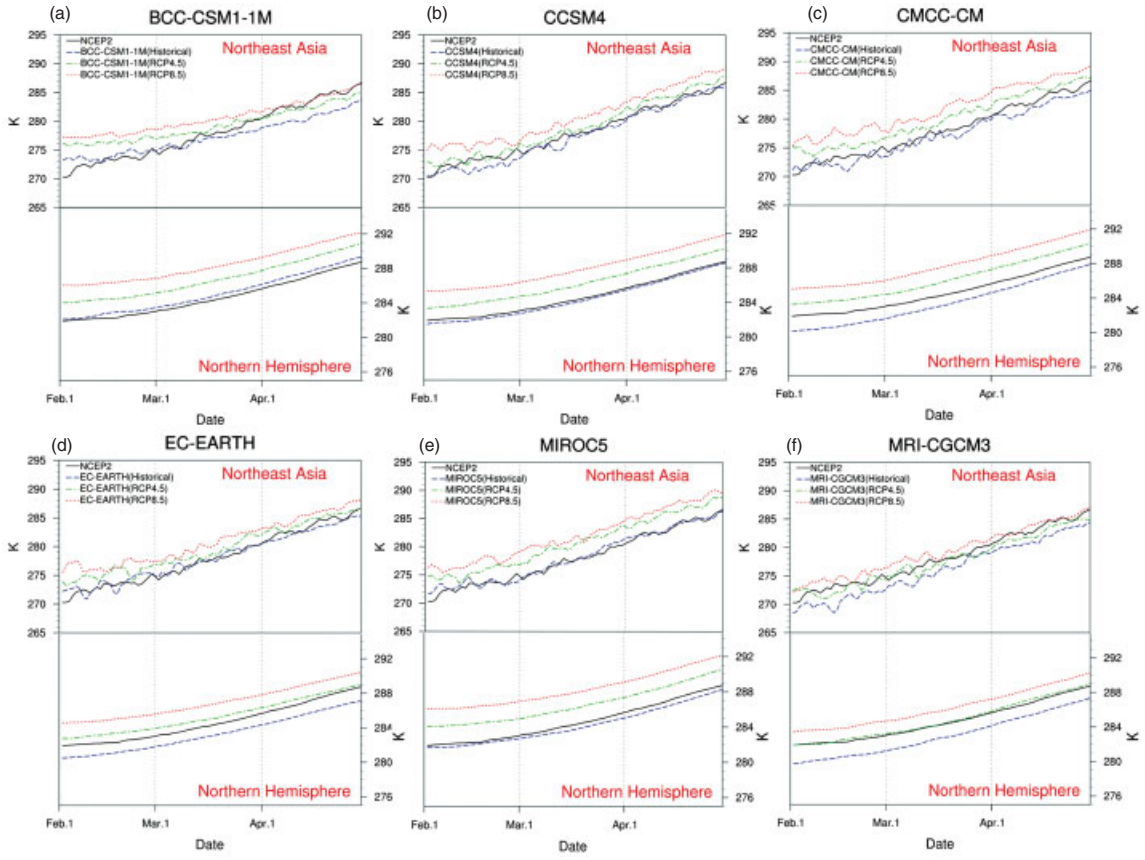

Figure 3. Daily mean temperature (K) derived from NCEP reanalysis 2 data (averaged over 1986–2005, black solid line), and Historical (averaged over 1986–2005, blue dashed line), RCP4.5 (averaged over 2071–2090, green dash-dotted line), and RCP8.5 (averaged over 2071–2090, red dotted line) simulations over Northeast Asia and the Northern Hemisphere from 1 February to 30 April.

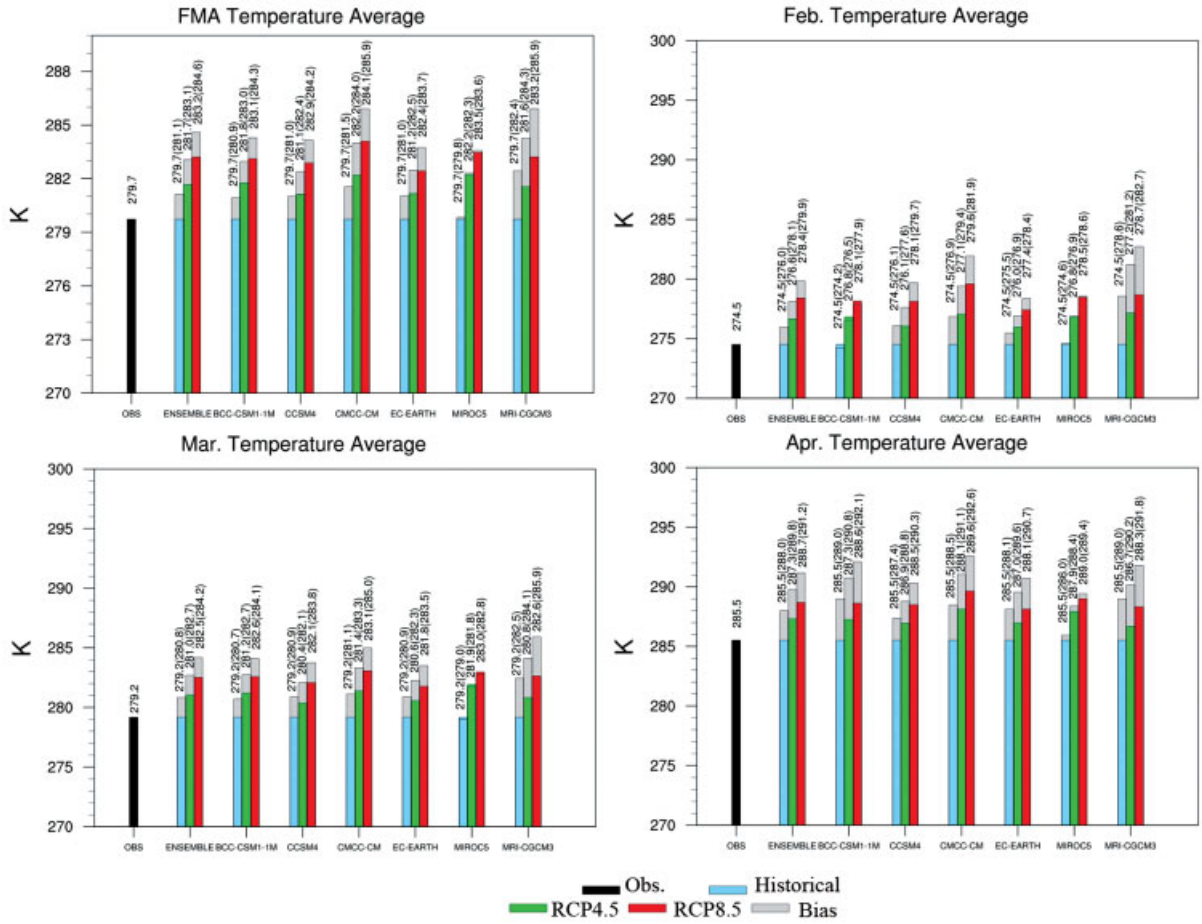

Figure 4. Average temperatures derived from observation (for 1986–2005, black), and Historical (for 1986–2005, sky blue), RCP4.5 (for 2071–2090, green), and RCP8.5 (for 2071–2090, red) simulations during the flowering period (February–April). Unit is absolute temperature, K.

The average temperatures over Northeast Asia simulated under the RCP4.5 and RCP8.5 scenarios are expected to increase by 2090 about 2.0 and 3.5 K, respectively, compared to the Historical simulation which is lower than the Northern Hemisphere average increase of 2.8 and 4.9 K, respectively. The amounts of increase associated with the RCP scenarios from BCC-CSM1-1M, CCSM4, EC-EARTH, MIROC5, and MRI-CGCM3 generally increase with increasing latitude (e.g. Oh *et al.*, 2004; Im *et al.*, 2008), whereas CMCC-CM shows a relatively large increase over land, including the Korean Peninsula.

According to the daily temperature time series, the temperature increase is highest for the RCP8.5 simulations, followed by the RCP4.5 and Historical simulations (Figure 3). The temperature change in February is larger than that in April in the RCP scenario simulation. Im and Ahn (2011) and Ohashi and Tanaka (2010) attributed such increase to the snow-albedo feedback. According to their analysis, melted snow in high elevation under warming leads to reduced surface albedo, which increases solar radiation absorption. As a result, the rising trend in temperature during February–April over Northeast Asia and the Northern Hemisphere is 0.17 and 0.09 K day^{-1} in Historical simulations, 0.16 and 0.08 K day^{-1} in RCP4.5 and 0.15 and 0.08 K day^{-1} in RCP8.5, respectively. The temperature tendency over Northeast Asia is similar with that over the Northern Hemisphere, but its features are more complex and variable due to topographical factors (Gao *et al.*, 2008; Im and Ahn, 2011). Therefore, a statistically downscaled temperature change at the *in-situ* observational sites over South Korea, which has diverse topographical features, and the accompanying local subsequence change are analysed.

3.2. Change of regional temperature

Figure 4 shows the average early spring temperatures over South Korea derived from the observation, and the Historical, RCP4.5, and RCP8.5 simulations. Systematic biases in individual models are estimated and eliminated based on the method suggested by Ahn *et al.* (2012). The estimated mean biases for early spring are 1.2, 1.3, 1.8, 1.3, 0.1, and 2.7 K for BCC-CSM1-1M, CCSM4, CMCC-CM, EC-EARTH, MIROC5, and MRI-CGCM3, respectively. By applying MME to the downscaled data after bias removal, ensemble data representing each scenario are produced and examined. The temperatures over South Korea at RCP4.5 and RCP8.5 are expected

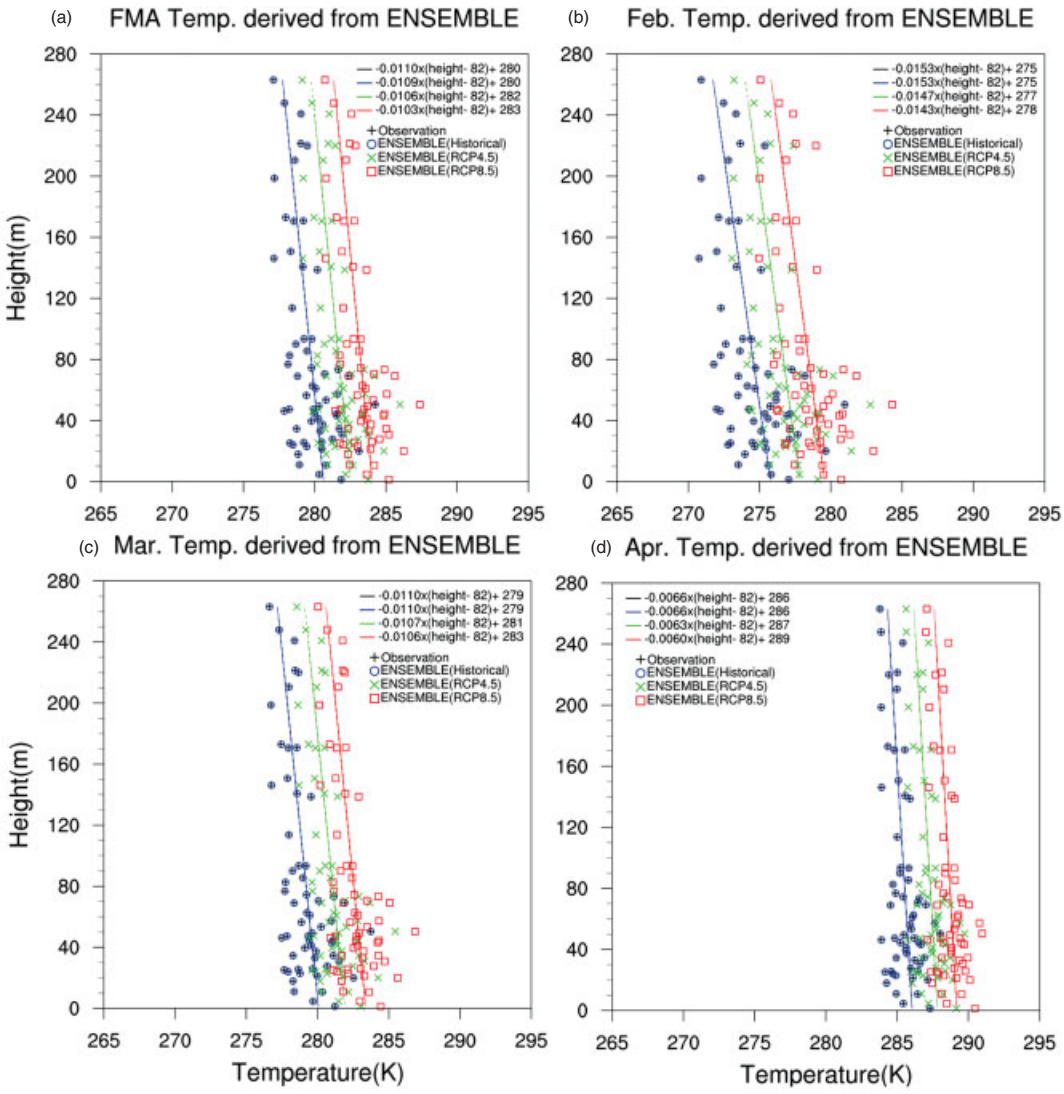

Figure 5. Scatter plots of the altitude of 59 stations against temperature at the corresponding locations for the flowering period (February–April).

to increase about 2.0 and 3.5 K by 2090 compared to the Historical simulation (279.7 K), respectively. The temperature changes are similar with the mean increments over Northeast Asia as shown in Figure 2. The increments in temperature are 2.1 and 3.9 K in February, 1.8 and 3.3 K in March, and 1.8 and 3.2 K in April under RCP4.5 and RCP8.5 scenarios, respectively, compared to a temperature increase of 1.8 K in the early spring (February–March) observed during the half century from 1954 to 2004 in South Korea (Jeong *et al.*, 2011).

The warming with respect to elevation is investigated in order to assess the altitude dependency of temperature change (Figure 5). The temperature decreases with increasing altitude in the Historical simulation, and this pattern continues for the RCP4.5 and RCP8.5 scenarios. Furthermore, the lapse rate in February is steeper than that in April when the air is more humid. The temperatures simulated under the RCP4.5 and RCP8.5 scenarios tend to increase uniformly regardless of the altitude compared with the Historical simulation. In fact, the temperatures at high elevation relatively increase slightly more than those at low altitude. For example, rising mean temperatures at 1 km under the RCP4.5 and RCP8.5 scenarios are 0.3 and 0.6 K, respectively, higher than the values at the surface, which are statistically significant at the 99% confidence level based on Student's t-test. This result corresponds with the result of Im and Ahn (2011), and is attributed to the snow-albedo feedback mechanism. However, the elevation dependency of the observation over this region appears to be quite limited because most of the stations are located below 280 m.

The spatial distributions of the mean temperature derived from the observation and simulations are presented in Figure 6. In the observation, the temperature is relatively low in high latitude and mountainous regions, and high in low latitude and flat areas due to the topographic effect. The Historical simulation well captures the topographical signals appearing in the observation. However, the temperatures simulated under the RCP4.5

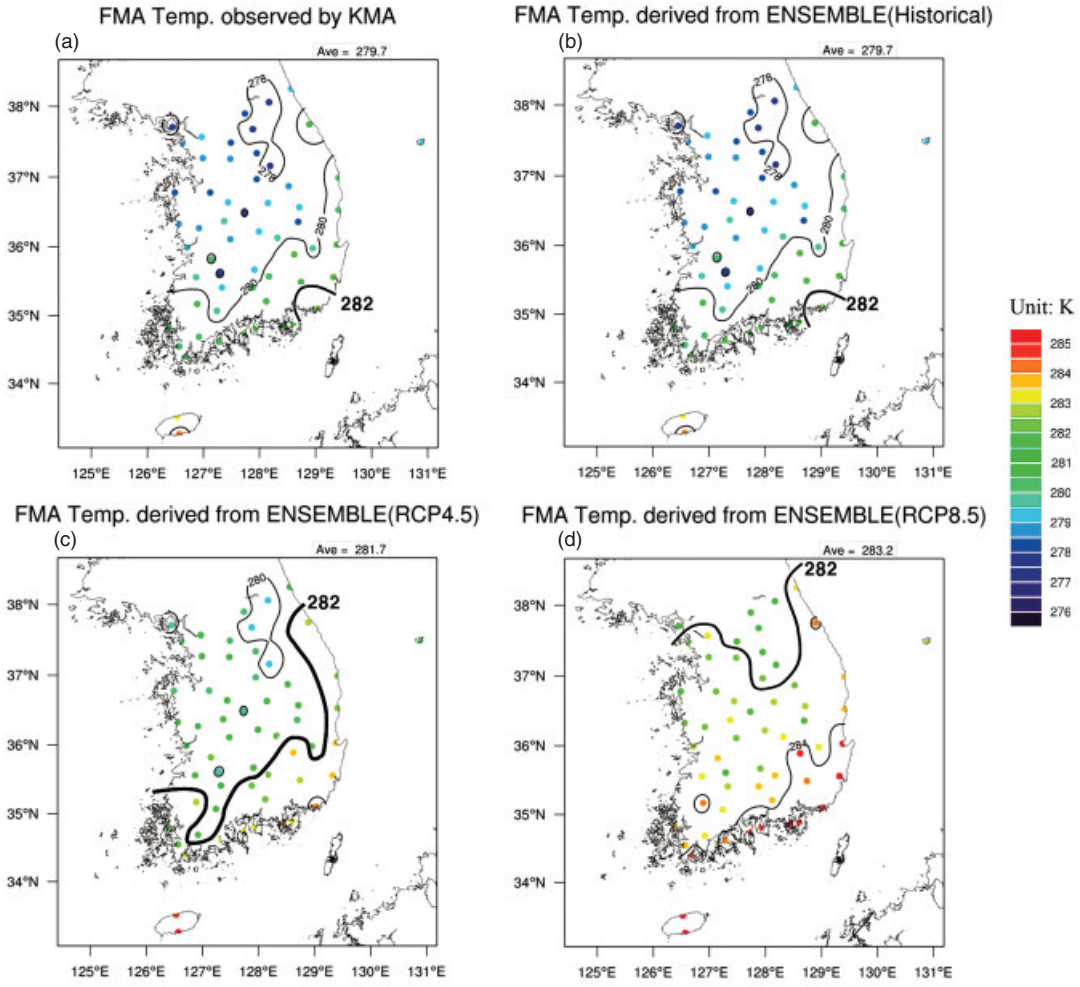

Figure 6. Spatial temperature distribution derived from observation (for 1986–2005, a), and Historical (for 1986–2005, b), RCP4.5 (for 2071–2090, c), and RCP8.5 (for 2071–2090, d) simulations for the flowering period (February–April). Unit is absolute temperature, K.

and RCP8.5 scenarios increase uniformly independent of the altitude compared with the Historical simulation, and maintain the topographical effect, even under climate change. In terms of the quantitative estimate, the 282 K line located around 35°N in the observation and Historical simulation is moved poleward by about 1°N and 2.5°N by 2090 to around 36°N and 37.5°N under the RCP4.5 and RCP8.5 scenarios, which approximately correspond to a northward moving speed of 0.01 and 0.03°N year^{-1}, respectively.

3.3. Change of cherry FFD

To estimate cherry FFD by the DTS method, the most suitable parameters in Equation 3 over the South Korea region are determined. In selecting the optimal parameters, we set 5-day interval for Ds from January 1 to February 26 and 4 kJ mol^{-1} intervals for E_a from 40 to 100 kJ mol^{-1}, and calculate the DTS with 192 combinations [12 (the number of Ds) × 16 (the number of E_a)]. Using each combination and the corresponding DTS, we estimate cherry FFD and calculate its root mean square error (RMSE) (Figure 7). According to the results, DTS has the lowest RMSE (2.67 days) when E_a is 76 kJ mol^{-1} and Ds is JD 47, and the highest RMSE (4.82 days) when E_a is 100 kJ mol^{-1} and Ds is JD 1. Thus, E_a of 76 kJ mol^{-1}, Ds of JD 47, and DTS of 18.8 are selected.

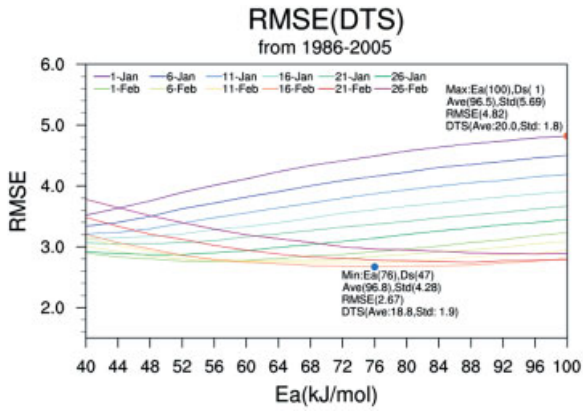

Figure 7. Changes in RMSE of cherry FFD according to the variation of E_a and Ds in the DTS method using observed temperature and FFD data from 1986 to 2005.

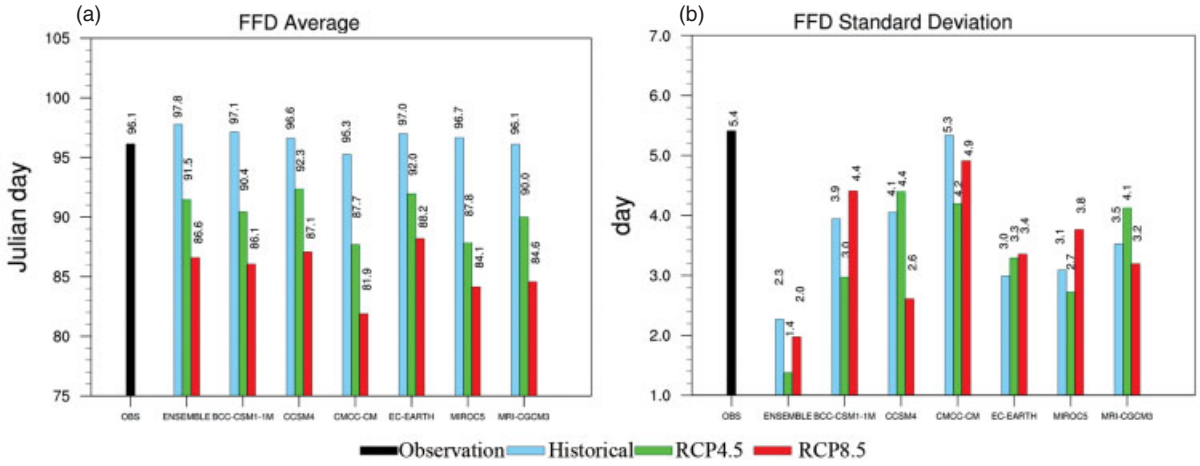

Figure 8. Average cherry FFD (left, Julian day) and standard deviation of FFD (right, day) derived from observation (for 1986–2005, black), and Historical (for 1986–2005, sky blue), RCP4.5 (for 2071–2090, green), and RCP8.5 (for 2071–2090, red) simulations.

Cherry FFD is estimated by applying the constants and DTS to the simulated temperature. Figure 8 shows the mean cherry FFD derived from the observation and climate model results. The average current FFD is JD 96.1, indicating that the cherry blossom generally flowers at the beginning of April. On the other hand, the cherry blossoms from the RCP4.5 and RCP8.5 simulations are expected to flower at the end of March by moving forward about 6.3 and 11.2 days, respectively, compared to the present. In other words, the increased temperature in February and March accelerates the growth rate of the cherry blossom and thereby advances the phenological spring. Our estimation for the change in FFD projected from the RCP8.5 simulation is 18 days less than the change suggested by Chung *et al.* (2009) and Yun (2006), who applied the two-step phenological model to the monthly SRES A2 simulation over the period 2011–2100. The difference is attributed to various factors such as the difference in temporal and spatial resolutions of the models, scenarios, initial and boundary conditions, and systematic bias from the uncertainty of the individual model. More specifically, however, our experimental result is distinct from that of other studies in several respects. First, the SRES A2 scenario was used in the previous studies, whereas the RCP scenarios were employed in this study. Several studies (e.g. IPCC, 2007a, 2007b; Lamarque *et al.*, 2011) insist that the SRES A2 scenario is similar with RCP8.5, and that the difference in scenarios therefore does not greatly affect the temperature increment. Second, the two-step phenological model was used for estimating cherry FFD in the previous study. A comparison of the previous and present phenological models reveals them to be basically similar in aspects of temperature accumulation, indicating no critical reason for such discrepancy. Third, the previously projected temperature change over South Korea had been estimated from the data simulated by a single model, ECHO-G (Min *et al.*, 2005, 2006), whereas in the present study it is obtained from the MME results, which increases the reliability of the prediction. Moreover, the previous studies did not eliminate the mean bias of the climate model results (Oh *et al.*, 2004; Kwon 2005), which resulted in a biased FFD estimation. In contrast, MME (e.g. Krishnamurti *et al.*, 1999; Peng *et al.*, 2002; Suh *et al.*, 2012) and statistical correction methods (e.g. Piani *et al.*, 2010; Haerter *et al.*, 2011; Ahn *et al.*, 2012) are adopted in this study to minimize the uncertainties contained in the previous experiments.

All cherry FFD derived from the Historical, RCP4.5, and RCP8.5 simulations, however, have lower variations than that of the observation (Figure 8). This is a common characteristic of climate predictions produced by models which underestimate the fluctuations of variables (e.g. temperature, precipitation) (Ines and Hansen, 2006).

The altitude dependency of cherry FFD changes is also assessed by investigating the cherry FFD changes with elevation (Figure 9). The observed cherry FFD at high elevation is delayed due to the low daily temperature. It is natural to assume that the FFD delays with increasing altitude in the RCP4.5 and RCP8.5 simulations will be similar to or slightly less than that of the Historical simulation as the lapse rates under the two scenarios are similar or slightly less than that of the Historical simulation (as shown in Figure 5). However, no regularities of FFD change with altitude according to scenarios are apparent, possibly because the flowers are also influenced by other factors such as day length, precipitation, and solar radiation, in addition to temperature (Diekmann, 1996; Tyler, 2001; Yeang, 2007).

The spatial distributions of cherry FFD derived from the observation and simulations are also investigated (Figure 10). The observed cherry FFD is later in high latitude and mountainous regions. In qualitative terms, the Historical simulation can capture the spatial pattern of the observation, but in quantitative terms, the estimate is an average of 1.2 days later than the observation. The FFDs from the RCP4.5 and RCP8.5 simulations are uniformly advanced in time over all stations compared

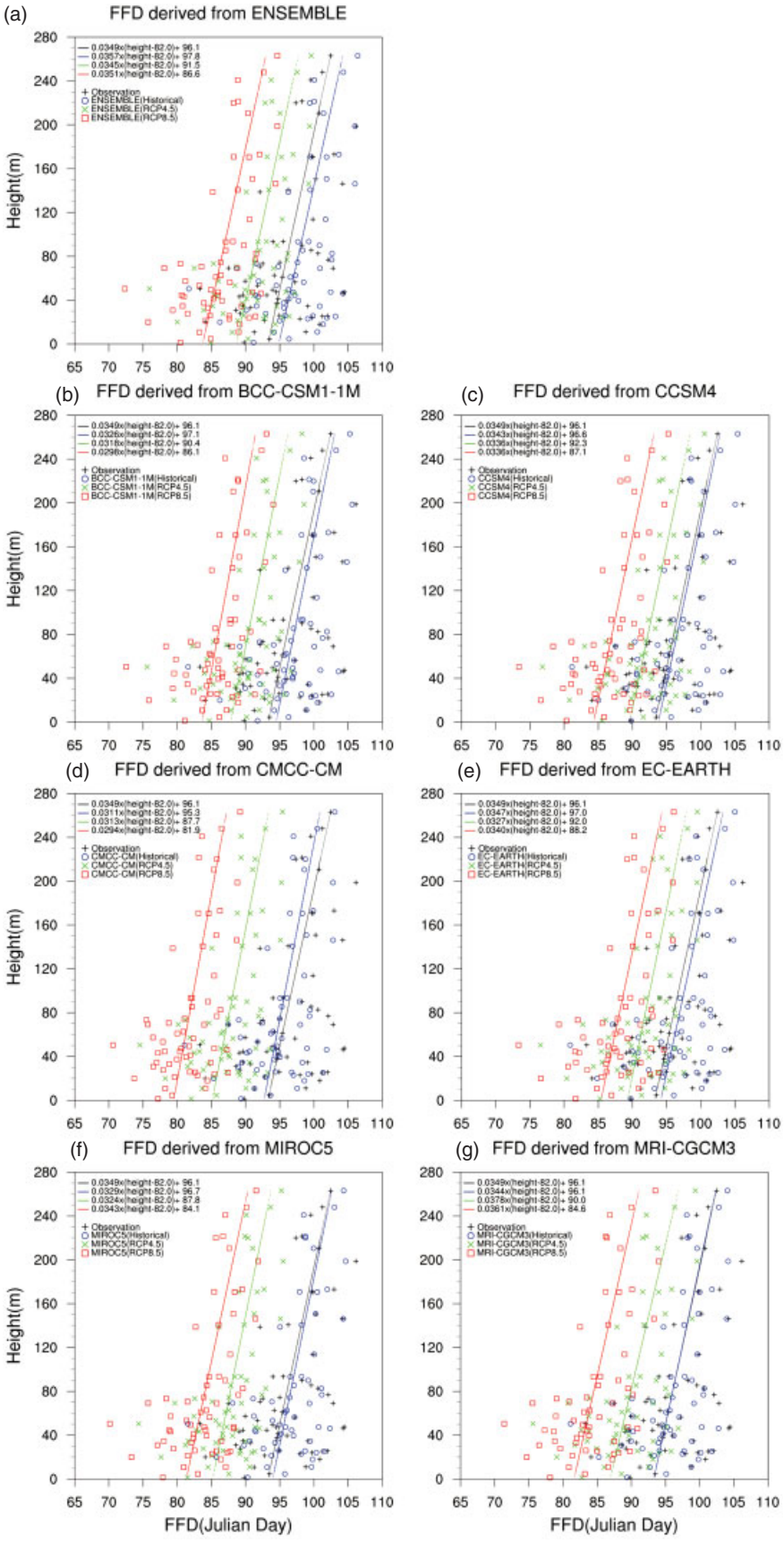

Figure 9. Scatter plots of the altitude of 59 stations against cherry FFD at the corresponding locations for the flowering period (February–April).

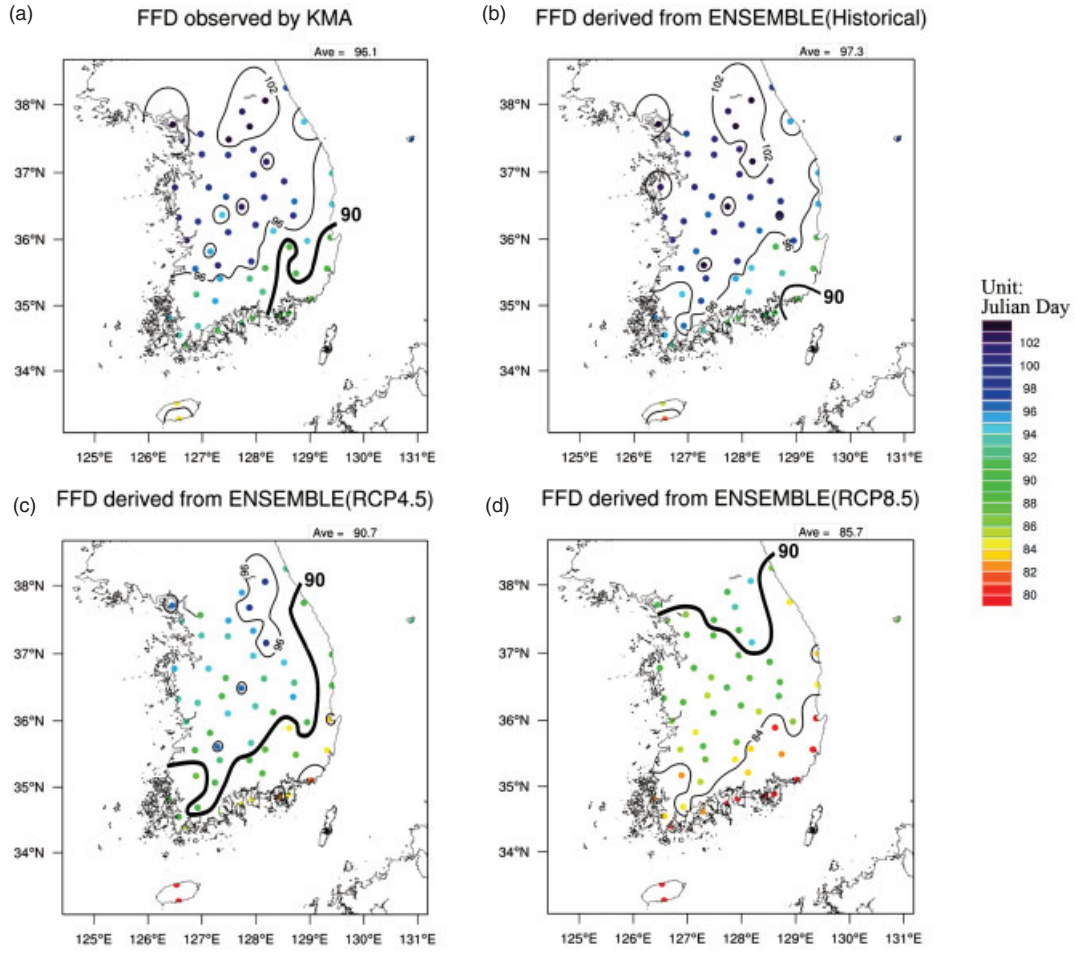

Figure 10. Spatial distribution of cherry FFD derived from observation (for 1986–2005, a), and Historical (for 1986–2005, b), RCP4.5 (for 2071–2090, c), and RCP8.5 (for 2071–2090, d) simulations for the flowering period (February–April). Unit is Julian day.

with the Historical simulation. Especially, FFD under the RCP8.5 scenario is advanced by 11.6 days compared to the Historical simulation. The changes of the 282 K line in temperature distribution, as shown in Figure 6, are remarkably consistent with the change of the 90-day line in the cherry FFD distribution, indicating that the current cherry FFD under the RCP4.5 and RCP8.5 scenarios moves north at a speed of 0.01 and 0.03°N year^{-1}, respectively.

4. Conclusion and summary

In this study, using 20th century Historical simulation (1986–2005), and RCP (2071–2090) 4.5 and 8.5 simulations based on AR5 scenarios and observation (1986–2005), early spring temperature changes over South Korea under global warming were statistically downscaled and accompanying cherry FFD variations were estimated.

On the basis of the projections, the temperatures over South Korea under the RCP4.5 and RCP8.5 scenarios were found to increase about 2.0 and 3.5 K by 2090, respectively. These increments were nearly uniform at all stations in South Korea, regardless of the elevation. Current isothermal lines are expected to move northward by about 1.0°N and 2.5°N by 2090, based on the RCP4.5 and RCP8.5 scenarios, respectively.

According to the cherry FFD analysis, rising temperature in February and March accelerated the growth rate of the cherry blossoms, which advanced FFD by about 6.3 and 11.2 days by 2090 under the RCP4.5 and RCP8.5 scenarios, respectively. This means that the current flowering of the cherry blossom over South Korea in early April is expected to flower at the end of March and the full bloom will occur by the beginning of April, at the latest, at the end of this century. The spatial movement of cherry FFD is expected to change consistent with that of temperature with a northward FFD movement speed of 0.01 and 0.03°N year^{-1} under the RCP4.5 and RCP8.5 scenarios, respectively.

The average yearly advance of the cherry FFD in the RCP4.5 and RCP8.5 simulations was 0.07 and 0.13 days year^{-1}, respectively, which was lower than the value of 0.18 days year^{-1} observed during the half century from 1954 to 2004 over South Korea (Jeong *et al.*, 2011). These results from RCP4.5 and RCP8.5 simulations are also 0.22 and 0.16 days year^{-1}, respectively, lower than the value of 0.29 days year^{-1} estimated with

the SRES A2 scenario (Yun, 2006; Chung *et al.*, 2009). This reduction in the advancement tendencies derived in this study, compared to that of Chung *et al.* (2009) and Yun (2006) obtained from the SRES A2 scenario, which is similar with RCP8.5, was primarily attributed to the non-elimination of any systematic bias in the model simulations of these previous studies, which caused an overestimation of the FFD change. Undoubtedly, the difference in several other factors such as phenological and climate models, temporal and spatial resolutions of the data and analysis period can also lead to a certain degree of discrepancy between the previous and current study results.

Although plant growth cannot be perfectly estimated using only temperature information due to the influence of many other environmental factors such as day length, precipitation, and solar radiation, this method can help to project potential variations of the local ecosystem in the present era of anthropogenic climatic change. The methodology used in this study to estimate cherry FFD can be applied to many different plants and crops in various aspects of growth response. For estimating regional warming, our results demonstrate the importance of eliminating the systematic bias inherently contained in the model simulation results in order to improve the prediction of future global climate changes.

Acknowledgements

This work was carried out with the support of Rural Development Administration Cooperative Research Program for Agriculture Science and Technology Development under Grant Project No. PJ009353 and Korea Meteorological Administration Research and Development Program under Grant CATER 2012-3083, Republic of Korea.

References

Ahn J-B, Hur J, Shim K-M. 2010. A simulation of agro-climate index over the Korean Peninsula using dynamical downscaling with a numerical weather prediction model, *Korean J . Agric. For. Meteorol.* **12**: 1–10(English Abstract).

Ahn J-B, Lee J, Im E-S. 2012. The reproducibility of surface air temperature over South Korea using dynamical downscaling and statistical correction. *J. Meteorol. Soc. Jpn.* **90**: 493–507, DOI: 10.2151/jmsj.2012-404.

Aono Y, Kazui K. 2008. Phenological data series of cherry tree flowering in Kyoto, Japan, and its application to reconstruction of springtime temperatures since the 9th century. *Int. J. Climatol.* **28**: 905–914, DOI: 10.1002/joc.1594.

Chung U, Jung J-E, Seo H-C, Yun JI. 2009. Using urban effect corrected temperature data and a tree phenology model to project geographical shift of cherry flowering date in South Korea. *Clim. Change* **93**: 447–463, DOI: 10.1007/s10584-008-9504-z.

Daly C, Helmer EH, Quinones M. 2003. Mapping the climate of Puerto Rico, Vieques and Culebra. *Int. J. Climatol.* **23**: 1359–1381, DOI: 10.1002/joc.937.

Diekmann M. 1996. Relationship between flowering phenology of perennial herbs and meteorological data in deciduous forests of Sweden. *Can. J. Bot.* **74**(4): 528–537, DOI: 10.1139/b96-067.

Dodson R, Marks D. 1997. Daily air temperature interpolated at high spatial resolution over a large mountainous region. *Climate Res.* **8**: 1–20, DOI: 10.3354/cr008001.

Gao X, Shi Y, Song R, Giorgi F, Wang Y, Zhang D. 2008. Reduction of future monsoon precipitation over China: comparison between a high resolution RCM simulation and the driving GCM. *Meteorol. Atmos. Phys.* **100**: 73–86, DOI: 10.1007/s00703-008-0296-5.

Gent PR, Danabasoglu G, Donner LJ, Holland MM, Hunke EC, Jayne SR, Lawrence DM, Neale RB, Rasch PJ, Vertenstein M, Worley PH, Yang Z-L, Zhang M. 2011. The Community Climate System Model Version 4. *J. Climate* **24**: 4973–4991, DOI: 10.1175/2011JCLI4083.1.

Haerter JO, Hagemann S, Moseley C, Piani C. 2011. Climate model bias correction and the role of timescales. *Hydrol. Earth Syst. Sci.* **15**: 1065–1079, DOI: 10.5194/hess-15-1065-2011.

Hazeleger W, Severijns C, Semmler T, Ştefănescu S, Yang S, Wang X, Wyser K, Dutra E, Baldasano JM, Bintanja R, Bougeault P, Caballero R, Ekman AML, Christensen JH, Hurk Bvd, Jimenez P, Jones C, Kållberg P, Koenigk T, McGrath R, Miranda P, Noije TV, Palmer T, Parodi JA, Schmith T, Selten F, Storelvmo T, Sterl A, Tapamo H, Vancoppenolle M, Viterbo P, Willén U. 2010. EC-Earth: a seamless Earth system prediction approach in action. *Bull. Am. Meteorol. Soc.* **91**: 1357–1363, DOI: 10.1175/2010BAMS2877.1.

Ho C-H, Lee E-J, Lee I, Jeong S-J. 2006. Earlier spring in Seoul, Korea. *Int. J. Climatol.* **26**: 2117–2127, DOI: 10.1002/joc.1356.

Im E-S, Ahn J-B. 2011. On the elevation dependency of present-day climate and future change over Korea from a high resolution regional climate simulation. *J. Meteorol. Soc. Jpn.* **89**: 89–100, DOI: 10.2151/jmsj.2011-106.

Im E-S, Ahn J-B, Kwon W-T, Giorgi F. 2008. Multi-decadal scenario simulation over Korea using a one-way double-nested regional climate model system. Part 2: future climate projection (2021–2050). *Clim. Dyn* **30**: 239–254, DOI: 10.1007/s00382-007-0282-5.

Ines AVM, Hansen JW. 2006. Bias correction of daily GCM rainfall for crop simulation studies. *Agric. For. Meteorol.* **138**: 44–53, DOI: 10.1016/j.agrformet.2006.03.009.

Intergovernmental Panel on Climate Change (IPCC). 2007a. Climate change 2001: The physical science basis. In *Contribution of Working Group I to the Fourth Assessment Report of the Intergovernmental Panel on Climate Change*, Solomon S *et al.* (eds). Cambridge University Press: Cambridge, UK.

Intergovernmental Panel on Climate Change (IPCC), 2007b. Towards new scenarios for analysis of emissions, climate change, impacts and response strategies, IPCC Expert Meeting Report.

Jeong J-H, Ho C-H, Linderholm HW, Jeong S-J, Chen D, Choi Y-S. 2011. Impact of urban warming on earlier spring flowering in Korea. *Int. J. Climatol.* **31**: 1488–1497, DOI: 10.1002/joc.2178.

Jung H-S, Choi Y, Oh J-H, Lim G-H. 2002. Recent trends in temperature and precipitation over South Korea. *Int. J. Climatol.* **22**: 1327–1337, DOI: 10.1002/joc.797.

Jung JE, Kwon EY, Chung U, Yun JI. 2005. Predicting cherry flowering date using a plant phenology model, *Korean J . Agric. For. Meteorol.* **7**: 148–155(English Abstract).

Kanamitsu M, Ebisuzaki W, Woollen J, Yang S-K, Hnilo JJ, Fiorino M, Potter GL. 2002. NCEP–DOE AMIP-II REANALYSIS (R-2). *Bull. Am. Meteorol. Soc.* **83**: 1631–1643, DOI: 10.1175/BAMS-83-11-1631.

Krishnamurti TN, Kishtawal CM, LaRow TE, Bachiochi DR, Zhang Z, Williford CE, Gadgil S, Surendran S. 1999. Improved weather and seasonal climate forecasts from multimodel superensemble. *Science* **285**: 1548–155, DOI: 10.1126/science.285.5433.1548.

Kwon W-T. 2005. Current status and perspectives of climate change sciences. *J. Korean Meteorol. Soc.* **41**: 325–336(English Abstract).

Lamarque J-F, Kyle GP, Meinshausen M, Riahi K, Smith SJ, van Vuuren DP, Conley AJ, Vitt F. 2011. Global and regional evolution of short-lived radiatively active gases and aerosols in the representative concentration pathways. *Clim. Change* **109**: 191–212, DOI: 10.1007/s10584-011-0155-0.

Menzel A, Dose V. 2005. Analysis of long-term time series of the beginning of flowering by Bayesian function estimation. *Metorol. Z.* **14**(3): 429–434, DOI: 10.1127/0941-2948/2005/0040.

Menzel A, Fabian P. 1999. Growing season extended in Europe. *Nature* **397**: 659, DOI: 10.1038/17709.

Min S-K, Legutke S, Hense A, Kwon W-T. 2005. Internal variability in a 1000-yr control simulation with the coupled climate model ECHO-G–I. Near-surface temperature, precipitation and mean sea level pressure. *Tellus A* **57**: 605–621, DOI: 10.1111/j.1600-0870.2005.00133.x.

Min S-K, Legutke S, Hense A, Cubasch U, Kwon W-T, Oh J-H, Schlese U. 2006. Internal variability in a 1000-yr control

simulation with the coupled climate model ECHO-G – I. Near-surface temperature, precipitation and mean sea level pressure. *J. Meteorol. Soc. Jpn.* **84**: 1–26, DOI: 10.2151/jmsj.84.1.

Mizuta R, Yoshimura H, Murakami H, Matsueda M, Endo H, Ose T, Kamiguchi K, Hosaka M, Sugi M, Yukimoto S, Kusunoki S, Kitoh A. 2012. Climate simulations using MRI-AGCM3.2 with 20-km grid. *J. Meteorol. Soc. Jpn.* **90**: 233–258.

Oh J-H, Kim T, Kim M-K, Lee S-H, Min S-K, Kwon W-T. 2004. Regional climate simulation for Korea using dynamic downscaling and statistical adjustment. *J. Meteorol. Soc. Jpn.* **82**: 1629–1643, DOI: 10.2151/jmsj.82.1629.

Ohashi M, Tanaka HL. 2010. Data analysis of recent warming pattern in the arctic. *SOLA* **6A**: 1–4, DOI: 10.2151/sola.6A-001.

Ohashi Y, Kawakami H, Shigeta Y, Ikeda H, Yamamoto N. 2012. The phenology of cherry blossom (*Prunus yedoensis* "Somei-yoshino") and the geographic features contributing to its flowering. *Int. J. Biometeorol.* **56**: 903–914, DOI: 10.1007/s00484-011-0496-4.

Ono S, Konno T. 1999. Estimation of flowering date and temperature characteristics of fruit trees by DTS method. *Jpn. Agric. Res. Q.* **33**: 105–108.

Peng P, Kumar A, den Dool HV, Barnston AG. 2002. An analysis of multimodel ensemble predictions for seasonal climate anomalies. *J. Geophys. Res.* **107**(d23): 4710, DOI: 10.1029/2002JD002712.

Piani C, Haerter JO, Coppola E. 2010. Statistical bias correction for daily precipitation in regional climate models over Europe. *Theor. Appl. Climatol.* **99**: 187–192, DOI: 10.1007/s00704-009-0134-9.

Scoccimarro E, Gualdi S, Bellucci A, Sanna A, Fogli PG, Manzini E, Vichi M, Oddo P, Navarra A. 2011. Effects of tropical cyclones on ocean heat transport in a high resolution coupled general circulation model. *J. Climate* **24**: 4368–4384, DOI: 10.1175/2011JCLI 4104.1.

Suh M-S, Oh S-G, Lee D-K, Cha D-H, Choi S-J, Jin C-S, Hong S-Y. 2012. Development of new ensemble methods based on the performance skills of regional climate models over South Korea. *J. Climate* **25**: 7067–7082, DOI: 10.1175/JCLI-D-11-00457.1.

Tyler G. 2001. Relationships between climate and flowering of eight herbs in a Swedish deciduous forest. *Ann. Bot.* **87**: 623–630, DOI: 10.1006/anbo.2001.1383.

van Vuuren DP, Edmonds J, Kainuma M, Riahi K, Thomson A, Hibbard K, Hurtt GC, Kram T, Krey V, Lamarque J-F, Masui T, Meinshausen M, Nakicenovic N, Smith SJ, Rose SK. 2011. The representative concentration pathways: an overview. *Clim. Change* **109**: 5–31, DOI: 10.1007/s10584-011-0148-z.

Watanabe M, Suzuki T, O'ishi R, Komuro Y, Watanabe S, Emori S, Takemura T, Chikira M, Ogura T, Sekiguchi M, Takata K, Yamazaki D, Yokohata T, Nozawa T, Hasumi H, Tatebe H, Kimoto M. 2010. Improved climate simulation by MIROC5: Mean states, variability, and climate sensitivity. *J. Climate* **23**: 6312–6335, DOI: 10.1175/2010JCLI3679.1.

Wielgolaski FE. 2003. Climatic factors governing plant phenological phases along a Norwegian fjord. *Int. J. Biometeorol.* **47**: 213–220, DOI: 10.1007/s00484-003-0178-y.

Wu T, Yu R, Zhang F, Wang Z, Dong M, Wang L, Jin X, Chen D, Li L. 2010. The Beijing climate center for atmospheric general circulation model (BCC-AGCM2.0.1): description and its performance for the present-day climate. *Clim. Dyn.* **34**: 123–147, DOI: 10.1007/s00382-009-0594-8.

Yeang H-Y. 2007. Synchronous flowering of the rubber tree (*Hevea brasiliensis*) induced by high solar radiation intensity. *New Phytologist* **175**(2): 283–289, DOI: 10.1111/j.1469-8137.2007.02089.x.

Yukimoto S, Yoshimura H, Hosaka M, Sakami T, Tsujino H, Hirabara M, Tanaka TY, Deushi M, Obata A, Nakano H, Adachi Y, Shindo E, Yabu S, Ose T, Kitoh A. 2011. Meteorological research institute-earth system model v1 (MRI-ESM1)–model description. *Tech. Rep. Meteorol. Res. Inst.* **64**: 88.

Yun JI. 2006. Climate change impact on the flowering season of Japanese cherry (*Prunus Serrulata* var. *spontanea*) in Korea during 1941–2100. *Korean J. Agric. For. Meteorol.* **8**: 68–76(English abstract).

Yun JI, Choi J, Yoon YK, Chung U. 2000. A spatial interpolation model for daily minimum temperature over mountainous regions. *Korean J. Agric. For. Meteorol.* **2**(4): 175–182(English abstract).

Yun W-T, Stefanova L, Krishnamurti TN. 2003. Improvement of the multimodel superensemble technique for seasonal forecasts. *J. Climate* **16**: 3834–3840, DOI: 10.1175/1520-0442(2003)016<3834:IOTMST>2.0.CO;2.